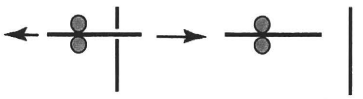

Fig. 8. Rope pulling.

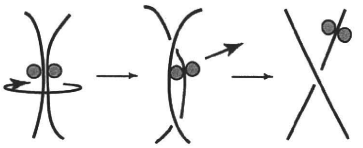

Fig. 9. Rope permutation + rope pulling (I).

in a plane, this skill is the free motion in the space above (or below) the plane. Rope moving is used to cross the two sections of the rope or to set one section close to another. When the two sections are intersected as shown in Fig. 11(a), one intersection is made. The description of the intersection can be written as

$$E_l - E_r \longrightarrow E_l - C_1^{\{+,-\}} - E_r.$$

When one section of the grasped rope approaches another, as shown in Fig. 11(b), the intersection is not created.

Rope moving strategy

Rope moving can be carried out by the three-dimensional motion of the robot hand.

## V. Analysis of Knot and Skill Synthesis

In this section, we analyze the feasibility of some knots based on synthesis of the individual skills described above. Then, a knot production process is proposed.

Wakamatsu et al. have proposed a process of knot manipulation based on four skills that consist of Reidemeister moves and rope crossing [6]. Although they described a systematic knot production process, the relationship between the knot production process and the required knot manipulation skills was not discussed.

In order to achieve actual knotting, it is necessary to consider not only the knot production process, but also the relationship between the production process and individual hand skills. For this reason, we propose the following analysis method.

**Analysis Method**

1) Represent a knot based on the description of the intersections that constitute the knot.
2) Unravel one intersection of the knot, starting from the intersection nearest the end of the rope.
3) Iterate 2) until the intersections disappear. As a result, a sequence of operations to remove the intersections is obtained.
4) Apply appropriate skills to the sequence, while following the sequence obtained in 3) in reverse.

By this process, the location and sign of each intersection is identified. As a result, it can be determined how to generate the intersections. This analysis can be applied not only to a knot generated by one rope, but also to a knot generated by one rope and one object and a knot generated by two ropes. Although the knot production process obtained by the proposed analysis method may not be optimal, this method can always provide one solution of the knot production process.

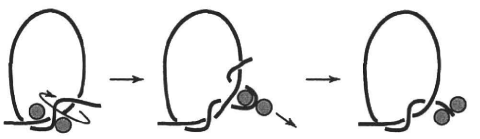

Fig. 10. Rope permutation + rope pulling (II).

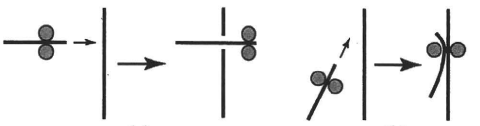

(a) (b)

Fig. 11. Rope moving.

### A. Knot Generated by One Rope

Here, we consider the description and production method of a knot generated by one rope. The start of the rope is located at the beginning of the rope (represented by $E_l$). The end of the rope is represented by $E_r$. As an example, here we analyze an "overhand knot".

Overhand Knot (Fig. 12(a))

An overhand knot is the simplest knot that is created on a rope. This knot prevents the rope unraveling.

Analysis of overhand knot

First, the description of the intersection in the overhand knot is

$$E_l - C_1^- - C_2^- - C_3^- - C_1^- - C_2^- - C_3^- - E_r. \text{ (Fig. 12(a))}$$

Next, removing one intersection ($C_3^-$), starting from the intersection near the end ($E_r$) of the rope, gives the following description of the intersections of the overhand knot:

$$E_l - C_1^- - C_2^- - C_1^- - C_2^- - E_r \text{ (Fig. 12(b))}$$

Iterating this operation until the intersections disappear yields the following description of the intersection

$$E_l - C_1^- - C_1^- - E_r \text{ (Fig. 12(c))}$$
$$E_l - E_r \text{ (Fig. 12(d)).}$$

The production process of the overhand knot can be obtained by following this process in reverse while considering the description of the intersections.

Production process of overhand knot

First, loop production is performed, and the intersection $C_1^-$ is created (Fig. 13(a)). Second, the intersection $C_2^-$ is produced. However, it is not effective to produce only the intersection $C_2^-$. By checking the final type of knot, it is found that two intersections should be made after the intersection $C_1^-$. In addition, the final intersection $C_3^-$ should pass under the rope. For these reasons, the state shown in Fig. 13(b) can be produced only by performing rope permutation

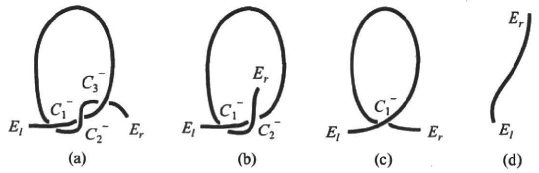


Fig. 12. Analysis of overhand knot.

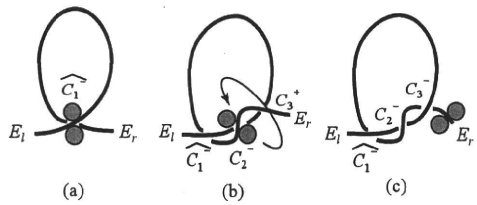


Fig. 13. Production process of overhand knot.

(Fig. 6(b)). Finally, using rope permutation and rope pulling (Fig. 10), the overhand knot is achieved, as shown in Fig. 13(c). The description of the intersections for the overhand knot production process can be represented by the following:

$$\widehat{E_l - E_r} \text{ (Fig. 12(d))}$$
$$E_l - \widehat{C_1^- - C_1^-} - E_r \text{ (Fig. 13(a))}$$
$$E_l - \widehat{C_1^- - C_2^- - C_3^+ - C_1^-} - C_2^- - C_3^+ - E_r \text{ (Fig. 13(b))}$$
$$E_l - C_1^- - C_2^- - C_3^- - \widehat{C_1^- - C_2^- - C_3^-} - E_r \text{ (Fig. 13(c))}$$

The eight knot and the stevedore's knot can be produced based on skill synthesis in the same way.

### B. Knot Generated by One Rope and One Object

In this section, we consider the knotting process of a knot generated by one rope and one object. As an example, we analyze a "half hitch".

Half hitch (Fig. 14)

The half hitch is one of the knots that make a connection between a rope and an object. Although it is an easy task to make this knot, the strength of the knot is very low. However, the strength can be increased by combining the half hitch with other knots.

Production process of half hitch

Here, we omit the intersection description of the half hitch. The left end and the right end of the rope are represented by $l_1$ and $l_2$, and the left end and the right end of the object are represented by $r_1$ and $r_2$. The description of intersections on the rope and the object is performed in the order of initial location.

First, the intersection $C_1^+$ is created by rope permutation (Fig. 14(b), (c)). Second, the rope is wrapped around the stick by rope moving to produce the intersection $C_2^+$ (Fig. 14(d)). Next, the intersection $\widehat{C_1^-}$ is made by loop production (Fig. 14(e)). Finally, the half hitch is finished by performing rope permutation twice and rope pulling once (Fig. 14(f), (g)).

A knot generated by two ropes can be considered in the same way; however, it is omitted in this paper.

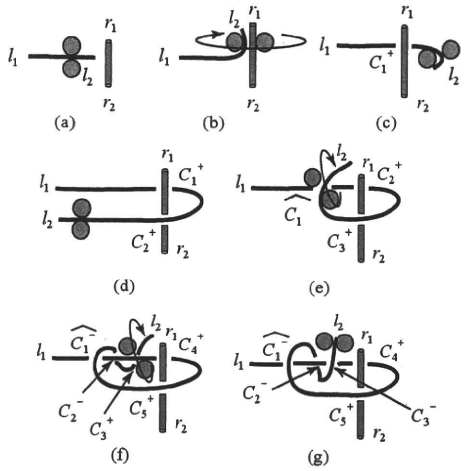


Fig. 14. Production process of half hitch.

## VI. Experiment

### A. Experimental system

The experimental system consists of a high-speed multi-fingered hand, high-speed tactile sensors, and a high-speed visual sensor.

The hand has three fingers and two wrist joints. The joints of the hand can be closed at a speed of 180 deg./0.1 s.

The tactile sensor measures the center position of a two-dimensionally distributed load, and the total load is measured within 1 ms. This sensor is used for grasp force control during rope permutation [1].

The visual sensor measures the center position $(x, y)$ and the angle of the principal axis of inertia within 1 ms. This sensor is used for the wrist-joint control during loop production in order to achieve robust control against rope deformation.

In order to prevent the rope from slipping on the fingers of the robot hand, a fingerstall is attached to each top link. One end of the rope is grasped by the robot hand, and the other end is held in a pulley so as to allow free up and down motion.

### B. Experimental Results

Fig. 16 and Fig 18 show sequences of continuous photographs of the knotting tasks (overhand knot and half hitch). The knotting strategy used was the one proposed in a previous paper [1].

Overhand knot

The experimental system is shown in Fig. 15. Fig. 16(a) $\sim$ (e) show loop production. In Fig. 16(f), the rope sections are pressed by the free finger to strengthen the contact state between the two sections. Fig. 16(g) $\sim$ (i) show rope permutation. Fig. 16(j) $\sim$ (l) show rope pulling.

Half hitch

The experimental system is shown in Fig. 17. In the initial state, the rope is wrapped around the object, as shown in Fig. 17. Fig. 18(a) $\sim$ (c) show loop production. In Fig. 18(d), the

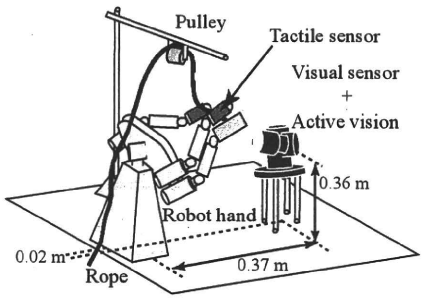


Fig. 15. Overall system for overhand knot production.

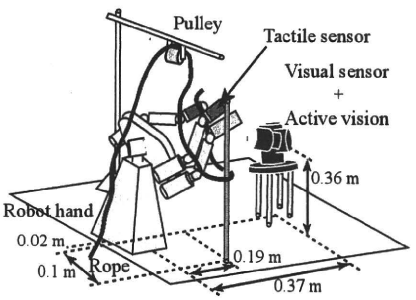


Fig. 17. Overall system for half hitch production.

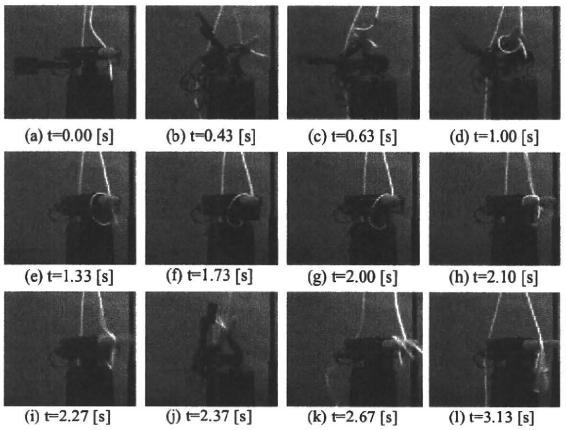


Fig. 16. Continuous photographs of overhand knot.

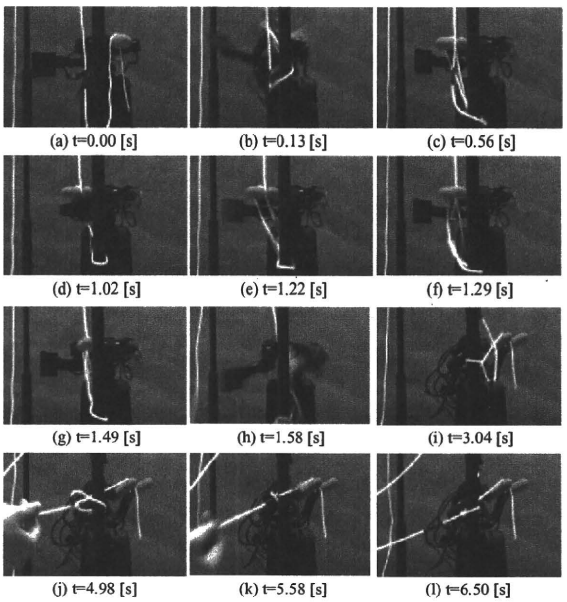


Fig. 18. Continuous photographs of half hitch production.

rope sections are pressed by the free finger to strengthen the contact state between the two sections. Fig. 18(e) $\sim$ (g) show rope permutation. Fig. 18(h) $\sim$ (i) show rope pulling. Finally, Fig. 18(j) $\sim$ (l) show additional rope pulling by a human hand to tighten up the knot.

These video sequences can be viewed on our web site [7].

## VII. Conclusions

First, to identify the necessary skills for knotting, we analyzed a knotting action performed by a human subject. As a result, we identified four skills.

Next, we proposed a method to produce a knot. The proposed method is based on a description of the intersections that constitute the knot, and it is described by the sequence of operations achieved using the four identified skills. We analyzed three types of knot: a knot generated by one rope, a knot generated by one rope and one object, and a knot generated by two ropes. These knots could be produced by the synthesis of the four skills. In addition, we also determined the relationship between the knot production process and the individual skills required by the robot hand in knot manipulation.

Finally, we demonstrated production of an overhand knot and a half hitch by using a high-speed multifingered hand system. In the future, we will attempt to apply our approach to other types of knots.

## References

[1] Y. Yamakawa, A. Namiki, M. Ishikawa and M. Shimojo, High-speed Manipulation of a Flexible Rope Using a Multifingered Hand and Visual and Tactile Feedback. *Proc. of 13th Robotics Symposia*, pp. 529–534, 2008 in Japanese.

[2] H. Inoue and M. Inaba, Hand-eye Coordination in Rope Handling, *Robotics Research: The First International Symposium, MIT Press*, pp. 163–174, 1984.

[3] T. Matsuno, T. Fukuda, and F. Arai, Flexible Rope Manipulation by Dual Manipulator System Using Vision Sensor, *Proc. IEEE/ASME Int. Conf. on Advanced Intelligent Mechatronics*, pp. 677–682, 2001.

[4] M. Saha and P. Isto, Motion Planning for Robotic Manipulation of Deformable Linear Objects, *Proc. IEEE Int. Conf. on Robotics and Automation*, pp. 2478–2484, 2006.

[5] T. Morita, J. Takamatsu, K. Ogawara, H. Kimura, K. Ikeuchi, Knot Planning from Observation, *Proc. IEEE Int. Conf. on Robotics and Automation*, pp. 3887–3892, 2003.

[6] H. Wakamatsu, E. Arai, and S. Hirai, Knotting/Unknotting Manipulation of Deformable Linear Objects, *International Journal of Robotics Research*, Vol.25, No.4, pp. 371–395, 2006.

[7] http://www.k2.t.u-tokyo.ac.jp/fusion/Knotting/

SICE Annual Conference 2008
August 20-22, 2008, The University Electro-Communications, Japan

# Grasping Force Control of Multi-fingered Robot Hand based on Slip Detection Using Tactile Sensor

Daisuke Gunji[3], Yoshitomo Mizoguchi[1], Seiichi Teshigawara[2],
Aiguo Ming[2], Akio Namiki[4], Masatoshi Ishikawa[2] and Makoto Shimojo[1]

[1]Graduate School of Electro-Communications, University of Electro-Communications, Tokyo, Japan
[2]Graduate School of Information Science and Technology, The University of Tokyo, Tokyo, Japan
[3]NSK Ltd, Emerging Techonologies R&D Department, Japan
[4]Department of Artificial System Sience ,Chiba University, Chiba, Japan

**Abstract:** To achieve a human like grasping with a multi-fingered robot hand, the grasping force should be controlled without using information from the grasped object such as its weight and friction coefficient. In this study, we propose a method for detecting the slip of a grasped object using the force output of Center of Pressure (CoP) tactile sensors. CoP sensors can measure the center position of a distributed load and the total load applied on the surface of the sensor, within 1 ms. These sensors are arranged on the fingers of the robot hand, and their effectiveness as slip detecting sensors is confirmed in tests of slip detection during grasping. Finally, we propose a method for controlling grasping force to resist tangential force applied to the grasped object using a feedback control system with the CoP sensor force output.

**Keywords:** hand, tectile sensor, slip detection

## 1. INTRODUCTION

In order for robots to achieve the same level of precision in manual operation that humans achieve, many researchers are working on highly versatile, multi-fingered robot hands that offer a high degree of freedom. A typical operation of hands is grasping objects. In the past, since it was assumed that robots would grasp specific objects, it was sufficient to use a simple gripper structure as a hand, and to set its grasping force to the required value. However, since each grasped object has a different coefficient of friction and weight, to achieve human-like grasping, it is necessary to set the grasping force appropriately for each object without being aware of this data in advance. Moreover, in order to grasp objects without damaging them, it is desirable to grasp them with the minimum force without slip. Various slip sensors have been proposed to achieve this kind of grasping ability [1].

In human grasping, Johansson et al [2][3] showed that localized slip between the skin and the grasped object is an important factor in adjusting grasping force. Maeno et al [4][5] proposed an elastic finger for distributed sensing using strain gauges with a curved surface, and showed that by imitating the method of grasping objects used by humans, it is possible to pick up any object for which the weight and friction coefficient is not known, at any speed. However, this approach involves the disadvantages of having to produce dedicated fingers, and the requirement for many strain amplifiers to support the arrays of strain gauges. Melchiorri [6] has proposed a method of controlling grasping force by detecting translation and rotational slip using force/torque sensors based on strain gauges, and distributed tactile sensors. However, with this approach the static friction coefficient of the object must be known. Furthermore, since distributed tactile sensors are used, wiring them into the robot is a problem. Ikeda et al [7] have proposed a method of controlling grasping force by measuring the degree of eccentricity of the contact surface using a camera. With methods such as this using vision, how to incorporate cameras in relatively small places such as hands is a problem. Furthermore, processing speed depends on the frame rate of vision, and it is generally difficult to achieve slip detection at high speeds.

This paper shows an approach to slip detection using thin, flexible, lightweight two-dimensional center of pressure tactile sensors (Center of Pressure sensors, hereafter "CoP sensors") [8][9] that can be mounted on a robot hand. CoP sensors can measure the center position of a distributed load applied to the surface of the sensor and the total load itself within 1(ms). Thus, rapid slip detection can be achieved. Furthermore, only four wires are needed, irrespective of the size of the sensor area, making it easy to mount them on a robot hand. This paper describes slip detection tests using CoP sensors and shows that slip can be detected immediately before it occurs based on the force output of the CoP sensors. Next we show that when force is added to a grasped object causing slip, it is possible to achieve grasp control to resist the force using a force control system with feedback from the force output of the CoP sensors. Finally we propose a method of grasping with optimal grasping force for the object even when its friction coefficient is not known, by adjusting the grasping force based on slip detection using the output of the CoP sensors.

## 2. STRUCTURE AND FEATURES OF THE SENSOR

### 2.1 Structure and Features of the CoP Sensor

CoP sensors can measure the center position of a distributed load and the total load itself [8][9]. The structure of the CoP sensor, as shown in Fig.1, consists of pres-



PR0001/08/0000-0894 ¥400 

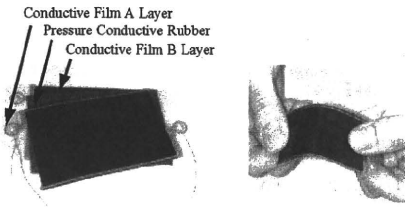


Fig. 1 Structure of CoP Sensor

sure sensitive material sandwiched between two sheets of conductive film, Layers A and B (upper and lower layers respectively). Both edges of the conductive film are electrodes, and we can derive the center position of the current distribution from the potential difference of the electrodes on both conductive film layers. Considering the pressure characteristic of pressure conductive material, it is possible to regard the center position of the current distribution as the center position of the load distribution, and the total current which flows circuit as the total load applied to the sensor.

Since CoP sensors consist of thin and flexible materials, they can be used arranged on curved surfaces. Furthermore, they find the center position of load distribution using the potential difference of the electrodes on both conductive film layers, so only four wires are required for the sensors, irrespective of their area, ensuring compact wiring. That is to say, CoP sensors have features that suit them to mounting on robot hands.

The arithmetic processing of the CoP sensors is achieved with simple analog circuits alone. Therefore, the time taken for calculation is very short, thereby achieving a high-speed response within 1(ms). Thus the sensors can be used directly in control loops of 1(kHz).

### 2.2 Output Characteristics of CoP Sensor

2.2.1 Position and Total Force Output

The position and the total force output characteristics of CoP sensor are shown in Fig.2 and Fig.3 respectively, when arranged on cylinder with diameters of 18(mm) equivalent to the finger-tip of the hand to use for an experiment. The point where pressure is applied and the output voltage of the sensor are in proportional relationship. The results show that as the pressure applied increases, the output of the sensor increases. In addition, with increasing and decreasing pressure the output differs, demonstrating hysteresis properties.

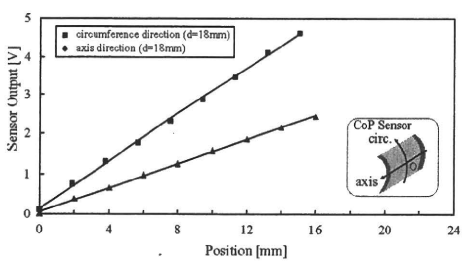


Fig. 2 Position output characteristics

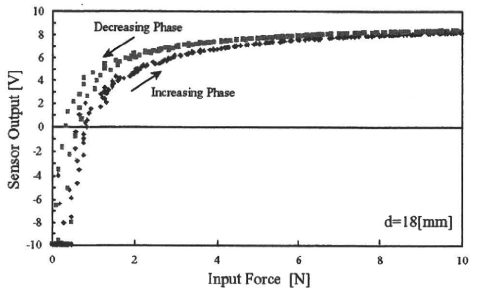


Fig. 3 Total force output characteristics

2.2.2 Slip Detection

We inspected behavior for tangential force of CoP sensor with the experimental system as shown in Fig.4.Firstly, the two fingers of the hand with the CoP sensors grasped an object.After grasping the object starts, the hand was made to maintain the same joint angle. The grasped object is connected to a DC motor by a wire, and was started to slip vertically downwards due to rotation of the DC motor. Vertical slip displacement of the grasped object was measured with a laser displacement sensor (Omron: ZX-LDA11-N) above the object. The outputs of the sensor and laser displacement sensor were input into a computer via an AD board (Interface: PCI-3168). The control cycle of the hand and the sensor output sampling cycle was 1(ms).

The results of the tests are shown in Fig.5. The figures show the slip displacement of the grasped object measured with a laser displacement sensor and the CoP sensor output (force output and position output). The change in CoP sensor position output due to the occurrence of slip is small with a maximum of 0.3(V). Immediately before slip displacement occurs, the total force output of the CoP sensors falls significantly (the shaded area of sensor force output in Fig.5). Thereafter at the stage where slip displacement is happening, the force output increases again, and during slip, complex changes are indicated. Since these characteristics may change depending on covering material, we performed the same experiment about some materials. As a result, the almost same characteristic was confirmed for all materials. Thus, It is thought that falling of total force output of CoP sensor can use slip detection.

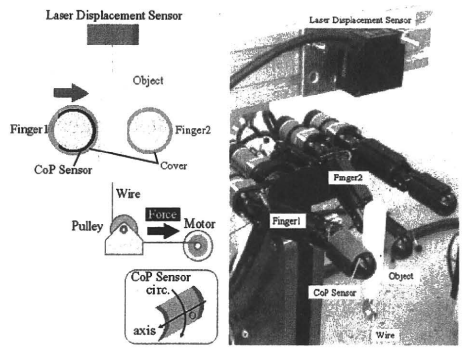


Fig. 4 Experimental system of slip detection on grasping

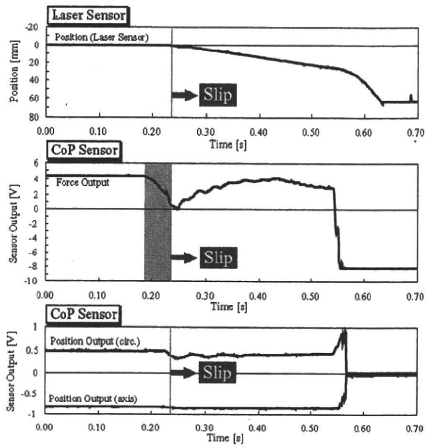


Fig. 5 Experimental result of slip detection on grasping

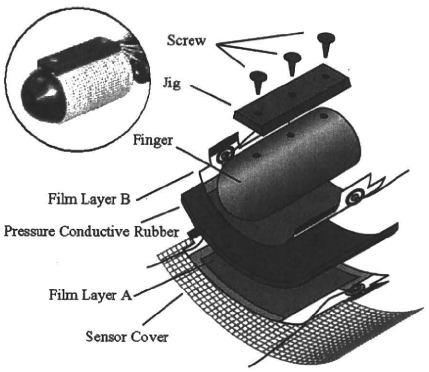


Fig. 6 Installation of CoP sensor

## 3. MULTI-FINGERED ROBOT HAND

In this research we used the high-speed three-fingered hand developed by Namiki et al [10]. This hand has three finger modules with two degrees of freedom, and it comprises joints that swivel the fingers on both sides. The finger modules incorporate an AC servomotor, harmonic drive, and encoder for driving the joints, and each joint is driven with a bevel gear.

Although small and light, this hand can open and close 180 degrees in 100(ms). In addition, it achieves high instantaneous output, obtaining greater grasping force than earlier hands. Furthermore, the hand has the superior characteristic in that backrush in the fingers overall is almost 0.

The maximum torque of the fingertip joints of the finger modules is 0.35(Nm), while that of the basal joints and swivel joints is 2.65(Nm). The control system feeds back the current target joint angle in relation to the target joint angle and sends commands regarding the torque of each joint using PD control. The control system was built on a PC with ART-Linux (kernel-2.4.22-0vl2.11ART) as the OS. The control cycle is 1(ms).

CoP sensors were mounted on each joint of the finger modules. The method used to mount the sensors on the finger modules is shown in Fig.6.

## 4. CONTROL OF A MULTI-FINGERED ROBOT HAND TO RESIST SLIP

### 4.1 The Basic Concept behind Grasping Force Control

From the test results in Section 2.2, it is clear that immediately before slip displacement occurs, the CoP sensors show changes in force output. Using this characteristic, we propose a method of control in which grasping force is increased when tangential force causing slip is detected. Hereafter, we will call the proposed control system anti-slip control.

In the test described in Section 2.2, vertical downward force was applied to the grasped object therefore there should be no change in normal force even at the stage when CoP sensor force output is changing. That is to say, force output of the CoP sensors actually shows a smaller value than for normal force. In relation to this, we considered control that achieves a certain sensor force output. If the sensor force output falls due to the occurrence of slip, control works to increase the force output. As a result, it is supposed that as an amount of slip force increases, the grasping force also increases through control.

In other words, with only a force control system that feeds back the CoP sensor force output, grasping force control that resists tangential force without any special control should be possible.

The proposed anti-slip control can be achieved with just a simple force control system, and no information about the grasped object whatsoever is required. However, if there is no margin in the target grasping force for the limits of friction, or if strong tangential force is applied, it is possible that increased grasping force from the control system will be insufficient and slip will occur.

### 4.2 Control System

As described in the previous section, with only a force control system that feeds back the CoP sensor force output, grasping force control that resists tangential force is possible. So damping control as shown in formula (1) was added to the PD control of the joint angle of the hand as anti-slip control.

$$\theta_{\mathrm{ref}} = \hat{\theta}_{\mathrm{ref}} + \hat{A} \int (V_{\mathrm{ext}} - V_{\mathrm{ref}})\, dt \qquad (1)$$

Here, $\hat{\theta}$ is the target joint angle, $\hat{A}$ is the coefficient, $V_{\mathrm{ext}}$ is the CoP sensor force output, $V_{\mathrm{ref}}$ is the target value for sensor force output, and $\theta_{\mathrm{ref}}$ is the new target joint angle. Normally, the force output of the CoP sensors and the relevant target values should be converted from voltage levels to force, but here for the sake of simplicity, the voltage levels themselves are used as is. Also for simplicity's sake, the position of the hand is not considered. Fig.7 shows the configuration of the control system.

### 4.3 Test Method

The hand grasped an object and when tangential force was applied to the grasped object, changes in the grasping force were measured.

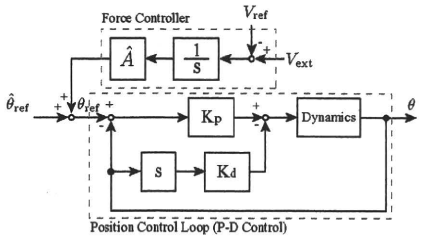


Fig. 7 Control system of muti-fingered robot hand

As shown in Fig.8 (a), an object with a load cell built into it was grasped by the fingertip joints of the hand.Anti-slip control was only applied to the basal joints of the fingers grasping the object. The target value of the sensor force output was $V_{\mathrm{ref}} = 3.0(V)$.

After the object was grasped, tangential force was applied by human hand to the grasped object. As shown in Fig.8 (b), tangential force was applied to the grasped object from three different directions in the tests, from above, from below, and from the front.

### 4.4 Test Result

Fig.9 shows the grasping force measured from the sensor force output and load cell with anti-slip control. The time shown shaded in the figure is when tangential force is applied. Furthermore, the numbers shown in circles indicate the direction of tangential force, corresponding to Fig.8(b). Irrespective of the direction in which the tangential force is applied, it is apparent that the load output of the CoP sensors falls significantly at the same time as tangential force is applied.

When anti-slip control is applied, grasping force increases significantly as soon as tangential force is applied. Furthermore, it is apparent that in all cases grasping force increases, irrespective of the direction of tangential force.

Therefore, the speed at which grasping force increases, in other words the responsiveness to the application of tangential force, changes with the gain of the control system. The influence of integration gain $\hat{A}$ in particular can be thought to be significant. The greater $\hat{A}$ is, the faster the response, but there is a greater possibility that instantaneous grasping force will be excessive, breaking the object.

The results of the tests show that with simple force control that feeds back the CoP sensor force output, it is possible to achieve grasping force control that resists tangential force.

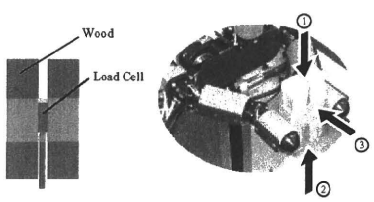


(a) Grasping object (b) Tangential force direction

Fig. 8 Experimental method

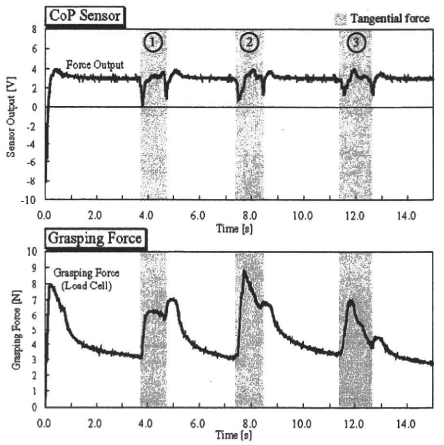


Fig. 9 Experimental result (anti-slip control)

## 5. MULTI-FINGERED ROBOT HAND GRIP CONTROL BASED ON SLIP DETECTION

### 5.1 Basic Concept

As one of the necessary sufficient conditions for a multi-fingered robot hand to be able to grasp an object in a still state there exists the condition that the power of each fingertip of the hand is within the friction cone [11]. Based on this, it is possible to prevent slip if control is performed so that fingertip power always remains within the friction cone. However, for this control a static friction coefficient is required as a parameter. In order to avoid restrictions on the objects that can be grasped, an approach is required that allows control even when the static friction coefficient is unknown. Therefore this paper proposes a method of control in which appropriate grasping force for the grasped object can be achieved even when the coefficient of friction and weight of the grasped object are unknown, using the force output of CoP sensors.

The basic concept of the proposed approach is as follows. When a hand grasps an object, if the grasping force is too weak, the object will slip. However, if this slip is detected and the grasping force is increased slightly, when the required grasping force is reached, slip no longer occurs. In the above process, all that is required is detection of slip and a corresponding increase in grasping force, and no information about the grasped object is required whatsoever. This approach is similar to the control method that humans may be supposed to use.

From the test results in Section 2.2.2it is clear that immediately before slip displacement of the grasped object occurs, the force output of the CoP sensors falls. Therefore, we propose a control method that regards this change in output as occurrence of slip, and increases the grasping force with a target in accordance with the occurrence of slip. With the proposed method, grasping force is controlled based only on sensor output, so no information about the grasped object such as the coefficient of friction is required whatsoever. Furthermore, since changes in sensor output can be obtained immedi-

ately before slip displacement occurs, if the hand operates fast enough, it should be possible to adjust grasping force before slip displacement occurs in most cases.

### 5.2 Control Method

The basic control system is the anti-slip control proposed in Section 4. Here, grasping force is adjusted by changing the target value for sensor force output $V_{\mathrm{ref}}$ in relation to the sensor output. Hereafter, we will simply call the target value for sensor force output $V_{\mathrm{ref}}$ the "target valu".

In the proposed method, a low value is first set for $V_{\mathrm{ref}}$, and grasping of the object starts. After grasping starts, $V_{\mathrm{ref}}$ is changed in accordance with formulas (2) and (3). $\Delta t$ is the control cycle.

When $V_{\mathrm{ref}}(t) - V_{\mathrm{ext}}(t) > V_{\mathrm{th}}$

$$V_{\mathrm{ref}}(t+\Delta t) = V_{\mathrm{ref}}(t) + K_{\mathrm{fp}}\{V_{\mathrm{ref}}(t) - V_{\mathrm{ext}}(t)\} \quad (2)$$

When $\dot{V}_{\mathrm{ext}} < c$ and $V_{\mathrm{ref}}(t) - V_{\mathrm{ext}}(t) > 0$

$$V_{\mathrm{ref}}(t+\Delta t) = V_{\mathrm{ref}}(t) - K_{\mathrm{fd}}\dot{V}_{\mathrm{ext}} \quad (3)$$

Here, $V_{\mathrm{th}}(>0)(V)$ and $c(<0)(V/s)$ are appropriate threshold values, and $K_{\mathrm{fp}}$ and $K_{\mathrm{fd}}$ are coefficients.

It can be said that the smaller the threshold value $V_{\mathrm{th}}$ and c in each conditions, the greater the sensitivity to slip. However, if the threshold value is too low, even if slip is not occurring, the target value will be increased, and the grasping force will be excessive. In addition, since the bigger the coefficients $K_{\mathrm{fp}}$ and $K_{\mathrm{fd}}$, the faster the target value is increased, it is possible to reduce the occurrence of slip displacement, but at the same, the possibility that grasping force becomes excessive also increases. Therefore, it is necessary to set appropriate values for these parameters, taking into account the responsiveness of the multi-fingered robot hand used for grasping.

### 5.3 Test Method

We tested the proposed control method on the multi-fingered robot hand, grasping an object for which the coefficient of friction and mass were unknown. The experimental system is shown in Fig.10.

The grasped object is a plastic bottle with water in it. By changing the amount of water in the bottle, its weight was set at 100(g), 150(g), and 200(g), and testing was conducted with each weight. Slip displacement of the bottle was measured with a laser displacement sensor (Omron: ZX-LDA11-N) above the object. The outputs of the sensor and laser displacement sensor were input into a computer via an AD board (Interface: PCI-3168). The control cycle of the hand and the sensor output sampling cycle was 1(ms).

First, the robot hand was made grasp the plastic bottle held by a human. After the hand grasped the bottle, the human let go of it so that only the hand was holding it.

Grasping control was only applied to the basal joints of the fingers grasping the bottle. Slip-resistant mesh (approx. 1(mm) lattice, thickness 0.5(mm)) was used to coat the surface of the sensors. The initial target value was $V_{\mathrm{ref}} = 6.0(\mathrm{V})$. The sensor force output voltage

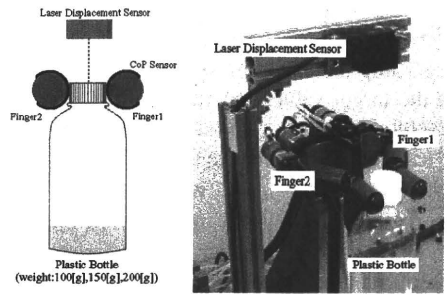


Fig. 10 Experimental system of grasping force control

Table 1 Experimental result of grasping force control

| | Weight | | |
|---|---|---|---|
| | 100 (g) | 150 (g) | 200 (g) |
| $V_{\mathrm{ref}}$ (V) | -0.24 | 1.4 | 3.7 |
| $V_{\mathrm{ref}}$ (Min) (V) | -1.5 | 1.0 | 3.5 |
| Slip (mm) | 0.54 | 1.4 | 2.5 |
| Adjustment time (s) | 0.60 | 1.09 | 0.83 |

when unloaded was -8.0 V. The various parameters were $V_{\mathrm{th}} = 1.0(\mathrm{V})$, $c = -30.0(\mathrm{V/s})$, $K_{\mathrm{fp}} = 3.0 \times 10^{-3}$, and $K_{\mathrm{fd}} = 5.0 \times 10^{-4}$.

Separately from the above test, we also examined the minimum grasping force that can be used to grasp the same object as in the test above without slip, in order to evaluate the proposed control method. Using the anti-slip control proposed in Section 4.we repeatedly changed the target value Vref in increments of 0.5 V for each weight of the grasped object until the hand grasped it without slip. The results for the minimum necessary grasping force were target values of -1.5 V (100 g), 1.0 V (150 g), and 3.5 V (200 g) respectively.

### 5.4 Test Results

Fig.11 shows the slip displacement of the grasped object with weight of 100(g), the sensor force output, and the target value. Table 1 shows the grasped object with weights of 150(g) and 200(g), with the target grasping force at the point when stable grasping was achieved $V_{\mathrm{ref}}$(V), the minimum necessary grasping force $V_{\mathrm{ref}}$ (Min) (V), the displacement that occurred up to stable grasping, and the time required up to that point.

The results of the test show that for all weights of object, grasping force was adjusted in accordance with the weight of the object using the proposed control method. When slip displacement and sensor force output are compared, the force output of the sensors falls significantly when slip displacement occurs, and the target value is increased accordingly. Furthermore, in all cases, adjustment of grasping force was performed in about 1(s). The slip displacement from the start of grasping to stable grasping is 0.5(mm) (100(g)), 1.4(mm) (150(g)), and 2.5(mm) (200(g)) respectively, and the heavier the object, the greater the slip displacement that occurs before stable grasping is achieved.

### 5.5 Discussion

Regarding the stable grasping state in the test results, when the target values obtained with the proposed control method and the minimum grasping force found in other tests are compared, the values are somewhat greater for objects of 100(g), but with objects of 150(g) and 200(g), values that largely match were obtained. Furthermore, the time required from the start of grasping to when grasping force was adjusted and stable grasping was achieved is short at 1(s). Even under the stringent conditions in this test when the object was passed in midair and the force was changed suddenly, stable grasping was achieved with relatively little slip displacement.

## 6. CONCLUSIONS AND FUTURE WORKS

### 6.1 Conclusions

In this paper we proposed an anti-slip control method using these characteristic force output changes, and confirmed the effectiveness of the proposed method through testing. Furthermore, we proposed a method of adjusting grasping force in response to slip detected using sensor force output, and in testing using the proposed method, we showed that optimum grasping force can be obtained even when no information about the grasped object is known.

### 6.2 Future Works

The reasons for the occurrence of the characteristic changes in sensor force output immediately before slipping occurs must be clarified. In addition, by covering the sensor surface with appropriate material, it should be possible to infer the direction of slip of an object from changes in the sensor position output. We will confirm these matters in future testing.

This paper describes tests with a relatively simple grasping position, but the proposed control method can probably also be applied to more complex grasping positions such as power grasps. Therefore in future we will examine control methods that take grasping position into consideration, with the aim of achieving dexterous grasping similar to that of humans.

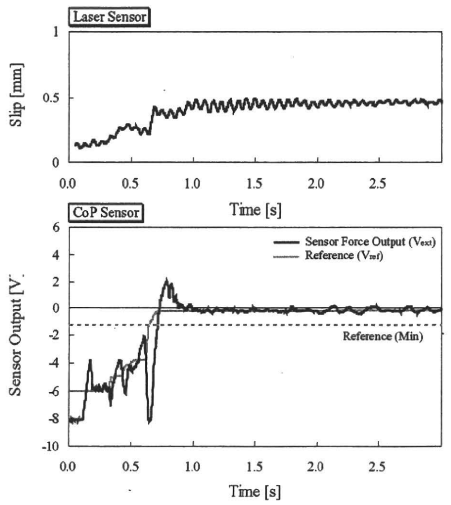


Fig. 11 Experimental result of grasping force control (weight: 100g)

## REFERENCES


[1] Y.Yamada, "Sensing Strategies before Grasping Part 2 Detection of Slip and Static Friction Coefficient Used to Acquire Information on Surface Roughnes", *Journal of the Robotics Society of Japan*, vol.11, no.7, pp.959-965, 1993.

[2] R.S.Johansson, G.Westling, "Roles of glabrous skin receptors and sensorimotor memory in automatic control of precision grip when lifting rougher or more slippery objects", *Exp Brain Res*, vol.56, pp.550-564, 1984.

[3] R.S.Johansson, G.Westling, "Signals in tactile afferents from the fingers eliciting adaptive motor responses during precision grip", *Exp Brain Res*, vol.66, pp.141-154, 1987.

[4] T.Maeno, S.Hiromitsu, T.Kawai, "Control of Grasping Force by Estimating Stick/Slip Distribution at the Contact Interface of an Elastic Finger Having Curved Surface", *Journal of the Robotics Society of Japan*, vol.19, no.1, pp.91-99, 2001.

[5] T.Kawai, Y.Hirano, T.Maeno, "Development of Strain Distribution Sensor Having Curved Surface for Grip Force Control", *The Japan Society of Mechanical Engineers.C*, vol.64, No.627, pp.4264-4270, 1998.

[6] Claudio Melchiorri, "Slip Detection and Control Using Tactile and Force Sensors", *IEEE /ASME Transaction on Mechatronis*, vol.5, no.3, pp.235-243, 2000.

[7] A.Ikeda, Y.Kurita, J.Ueda, Y.Matsumoto, T.Ogasawara, "Grip Force Control of the Elastic Body based on Contact Surface Eccentricity During the Incipient Slip", *Journal of the Robotics Society of Japan*, vol.23, no.3, pp.337-343, 2005.

[8] M.Ishikawa, M.Shimojo, "A Method for Measuring the Center Position of a Two Dimensional Distributed Load Using Pressure-Conductive Rubber", *The Society of Instrument and Control Engineers*, vol.18, no.7, pp.730-735, 1982.

[9] M.Shimojo, T.Araki, A.Ming, M.Ishikawa, "A ZMP Sensor for a Biped Robot", *Proc. IEEE Int. Conf. Robotics and Automation CD-ROM*, pp.1200-1205, 2006.

[10] A.Namiki, Y.Imai, M.Ishikawa and M.Kaneko, "Development of a High-speed Multifingered Hand System and its Application to Catching", *Proc.of IEEE/RSJ Int.Conf.on Intelligent Robots and Systems*, pp.2666-2671, 2003.

[11] T.Yoshikawa, Y.Yokokohji, A.Nagayama, "Object Handling by Tree-Fingered Hand Using Slip Motion", *Journal of the Robotics Society of Japan*, vol.10, no.3, pp.394-401, 1992.

SICE Annual Conference 2008
August 20-22, 2008, The University Electro-Communications, Japan

# Study of High Speed and High Sensitivity Slip Sensor
## Characteristic of conductive material

Seiichi Teshigawara*, Masatoshi Ishikawa**, Makoto Shimojo*

*Abstract*— **Slip detecting tactile sensors are essential to achieving a human-like gripping motion with a robot hand. Up until now, we have developed flexible, thin and lightweight center of pressure (CoP) sensor. The sensor, constructed of pressure conductive rubber sandwiched between two sheets of conductive film, is able to detect the center position of the load distribution and the total load. Recently, detection of initial slip has been shown to be possible. However the detection principles are unclear. Therefore, we carried out verification experiments of the slip detection properties of CoP sensor and the detection principle. In the results, we found a change in electrical conductivity produced with a shear deformation of the pressure conductive rubber. In this paper, we will discuss the slip detection properties of CoP sensor and detection principle. We will also apply these principle to describe the structure of high speed/high sensitivity slip sensor.**

## I. INTRODUCTION

With the aim of achieving a human-like robot hand, or one that is sperior to the human hand, much research have been carried out [1][2]. Even with eyes closed, humans can grip with minimum force an object with unknowns such as weight and coefficient of friction, etc. We are also able to perform smoothly such motions as handing the object off or setting it down. To achieve these motions with a robot hand requires tactile sensors having slip sense in addition to contact position and load.

So, up until now various slip sensors detecting slip have been proposed. Trembley et al. [3] developed a sensor, arranging acceleration sensors in sets of two inside a spherical silicon rubber with a projection called a "nib", that detected the vibrations which occur on the surface of the sensor as a result of initial slip. Son et al. [4] developed a sensor with four sheets of PVDF film arranged in a semi-circular silicon rubber tube that similarly detected the vibrations occurring from initial slip. Maeno et al. [5] developed sensor that lined up inside a curved elastic surface at regular intervals along a strain gauge. Shinoda et al. [6] proposed a slip sensor using Acoustic Resonant Tensor Cell (ARTC). The ARTC is composed of a resonance cavity within the elastic body and ultrasonic receiving probe, the slip direction stress is detected from changes in the ultrasonic wave resonance frequency.

As shown above, much research have been conducted regarding slip sensors. However, as of yet, a practical slip sensor does not exist. This is thought to be for the following causes. Firstly, there is the problem of reduction in size and weight. The space where sensors can be located for most robot hands is limited from the point of view of mechanism function. Accordingly, structures with devices embedded inside the fingers and thick sensors are undesirable. Secondly, there is the problem of wiring. When sensors using strain gauges or PVDF films are configured over a large area, it is necessary to increase the number of sensing elements and wires. Excessive wiring becomes a burden on the hand. Finally, there is the problem of response. Especially when cameras are used, response is dependent on the processing time of the data. Since a delay in response time increase the slip displacement of the object, high speed response is desirable.

Therefore, in this research, our goal is to develop thin, lightweight slip sensor with high speed response that could be installed on existing robot hands. Until now, we have carried out the research and development of center of pressure (CoP) tactile sensor for detecting two-dimensional load distribution with the following properties [7].

1) Flexible, thin(approximately 0.7 *mm*), lightweight(approximately 0.2 $g/cm^2$)
2) Wire saving(4*wires*)
3) High speed responsibility(1*ms*)

CoP sensor can detect the center of the load distribution and the weight of the load added to a surface. In recent experiments, it was found that these could be utilized as sensor to detect the initial slip as well [8]. However, the detailed detection mechanism is unclear. In this paper, we will simply mention the slip detection experiment using CoP sensor, and report on the slip detection properties and mechanism.

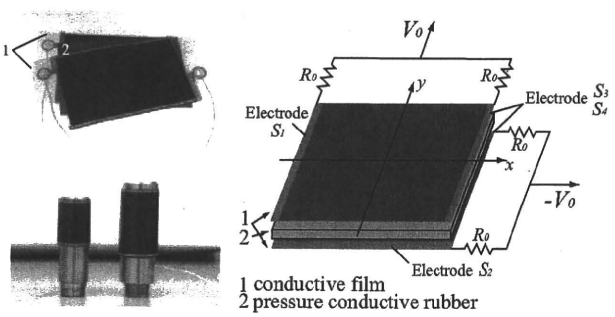


Fig. 1. Structure of CoP sensor

*Mechanical Engineering and Intelligent Systems, The University of Electro-Communications, 1-5-1 Chofugaoka, Chofu-shi, 182-8585 JAPAN
**Department of Information Physics and Computing, Graduate School of Information Science and Technology, The University of Tokyo, 7-3-1 Hongo, Bunkyo-ku, Tokyo 113-0033, Japan

## II. Slip Detection Using CoP Sensor

In this section, we show that CoP sensor can detect initial slip. So, we compared the CoP sensor load output with the gripping force measured by a load cell. The experimental apparatus utilized in this experiment is shown in Fig. 2. CoP sensors were arranged around two cylinders (diameter 18 *mm*), and fixed face-to-face. As in the figure, the object (plastic cylinder : 18 *mm*) was sandwiched by CoP sensors (Fig. 2-(1)), and this was connected by wire to the tension side load cell (we call "Loadcell(Z)" below). The gripping object was made to slip downward vertically (Fig. 2-(2)). Loadcell(X) in Fig. 2 denotes the normal vector force (gripping force) and Loadcell(Z) denotes the tangential force (tensile force). The slip displacement of the plastic cylinder was measured by a laser displacement sensor (resolution: 0.1*mm*). The results of this experiment are shown in Fig. 2. The graphs show, (a) CoP sensor load output, and (b) two load cells and laser displacement sensor output. From the laser displacement sensor output, the slip displacement occurs from the time of the vertical line shown on the graph.

We compared the CoP sensor load output with the grip force according to Loadcell(X). Looking at the grip force, its change was approximately 0.2 N and increasing just before the occurrence of slip displacement. Meanwhile, looking at the CoP sensor load output, there is a large decrease at the same time. The right side CoP sensor output decreased by approximately 4 V. According to the sensor load output characteristics, a decrease of approximately 1 N was produced. There was a decrease of approximately 1.3 N at the left side CoP sensor. We can say that the change is not one-sided because there was a simultaneous decrease in left and right outputs. Like this, in spite of the increase in the grip force, both sides CoP sensor load output decrease before slip displacement occurs. So, using these load output change of CoP sensor, it is possible to detect the start of slip (referred to as "initial slip").

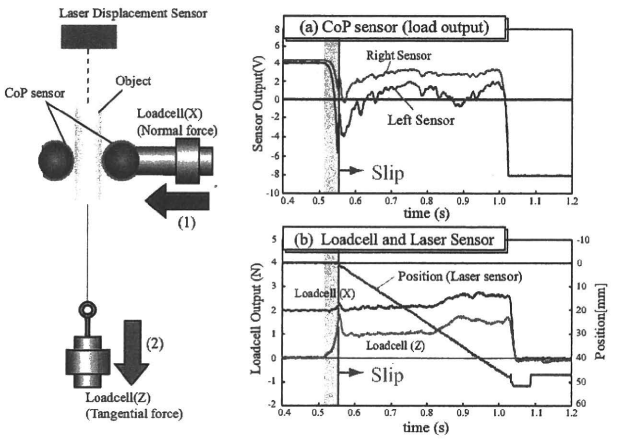


Fig. 2. Result of Slip detection experiment

From the above result, we expect that the change of CoP sensor load output is produced by the following phenomena. The following phenomena are believed to be produced in relation to the change in sensor load output (we call "slip output"). Looking at the colored area of Fig. 2-(a) and (c), CoP sensor load output begins to decrease at the same instant, and we find that the tangential force (Loadcell(Z) output) also begins to increase. From this, we expect that a shear deformation of pressure conductive rubber occurs inside the CoP sensor by the tangential force. some kind of internal change in the CoP sensor is produced in regard to the tangential force. Namely, that a shear deformation is produced in the pressure sensitive conductive rubber inside the CoP sensor by the tangential force. On the other hand, the change of CoP sensor load output is dependent on the electrical resistance change of the pressure conductive rubber. This indicates that there is some relationship between the shear deformation of the pressure conductive rubber and the change of electrical resistance. So, we conducted an experiment to observe the change of electrical resistance when pressure conductive rubber undergoes a shear deformation.

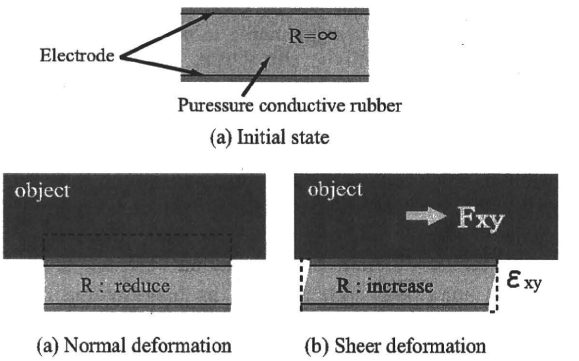


Fig. 3. Sheer deformation and Change of resistance

## III. Pressure Sensitive Conductive Rubber Shear Deformation Experiment

### A. Experimental Method

In this experiment, we reveal why CoP sensor output change when an object slip on CoP sensor. So, we inserted pressure conductive rubber electrodes, and measured the voltage between electrodes when it was made to undergo a shear deformation. The experimental apparatus is shown in Fig. 4. The electrodes (gold plated) were attached to acrylic plates, which were aligned facing each other (the circled area of Fig. 4). In the experiment, the electrodes were connected to a regulated power supply through a resistance of 1 $k\Omega$, and a voltage of 5 V was applied. The voltage (Va) was then stable at 5V. The X-stage installed on the right side of the experimental apparatus was activated, and the pressure conductive rubber (7 $mm^2$) was sandwiched between the electrodes (Fig. 4-(1)). This X-stage was equipped with a dedicated actuator, with a travel speed of 0.1 $mm/s$ and a positioning accuracy of 0.017 *mm*. Therefore, the quantity of the normal direction deformation of the pressure conductive rubber could be finely controlled. The X-stage was activated

again, and the normal direction load was increased. At this time, the voltage between electrodes was decreased from 5 V (load cell output : 0N) to 2 V (load cell output : approximately 1.7 N). From now on, this voltage is referred to as initial voltage ($V_i$). Next, the automatic stage installed on the left side was activated producing a shear deformation of pressure conductive rubber (Fig. 4-(2)). The automatic stage had a positioning accuracy of 0.012 *mm* and its speed could be adjusted from 1 $\mu m/s$ to 100 $mm/s$. The quantity of the shear deformation of the pressure conductive rubber could be measured by the laser displacement sensor (resolution 0.1 $\mu m$). In this experiment, the shear deformation of the pressure conductive rubber was set to 0.3 *mm*, and the three deformation speeds was set such as 0.05 $mm/s$, 0.1 $mm/s$, and 1 $mm/s$. The voltage between electrodes and the laser displacement sensor output were measured.

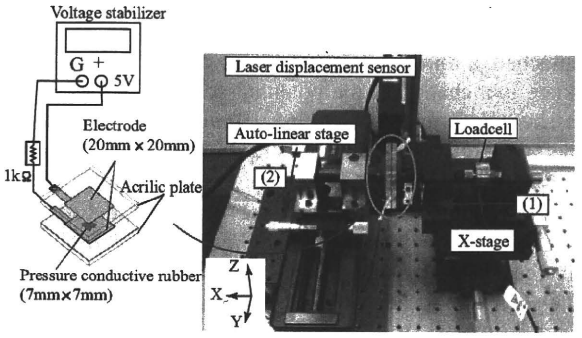


Fig. 4. Experimental system for deformation of pressure conductive rubber

### B. Experimental Results

The results of the experiment are shown in Fig. 5. Time(s) is along the horizontal axis and the voltage between electrodes and laser displacement sensor output (*mm*) are along the vertical axis. The voltage between electrodes increased, when the shear deformation of the pressure conductive rubber occurred. Taking the rise of the voltage at this point as $\Delta V$. Moreover, the voltage remained constant during sheer deformation of the rubber. When the sheer deformation stopped, the voltage gradually returned toward the initial voltage ($V_i$).

TABLE I
CHANGE OF VOLTAGE BETWEEN ELECTRODES

| Sheer deformation speed($mm/s$) | $\Delta V(V)$ |
|---|---|
| 0.05 | 1.4 |
| 0.1 | 1.6 |
| 1 | 2.1 |

## IV. DISCUSSION

*1) Change in Electrical Resistance of Rubber:* There was a large rise in the voltage between electrodes at the time of the shear deformation of the pressure conductive rubber. The rise of voltage indicated an increase in the electrical resistance of the rubber. As in the above hypothesis, we found that a change of electrical resistance was produced when a shear deformation of the rubber occurred. This fact

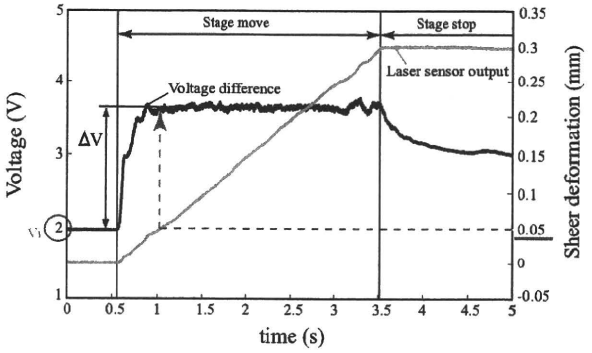


Fig. 5. The voltage difference between electrodes, sheer deformation speed : 0.1mm/s

was designated as a decrease in the load output of the CoP sensor. Looking at the result, the voltage difference $\Delta V$ raised more than 1.5 V with a shear deformation of only 0.05 *mm*. This time, there was a large increase in the electrical resistance of the pressure conductive rubber. This agrees with the large decrease of the CoP sensor load output that occurred before the change in the laser displacement sensor output utilized. Therefore, it is clear that the slip output of CoP sensor was generated by the change in electrical resistance of the pressure conductive rubber at the time of its shear deformation.

The rise in the electrical resistance of the pressure conductive rubber can be considered to be due to the following reasons. The pressure conductive rubber was a high polymer material primarily composed of silicon rubber with carbon particles uniformly distributed within. In an unloaded condition, because the carbon particles were separated from each other as in Fig. 6-(a), electric current would not flow. However, when the pressure was increased, the distribution of the carbon particles inside the rubber changed, and the carbon particles contacted each other as in Fig. 6-(b) forming a conduction route. when there is an increase in conduction routes due to contact of carbon particles in pressure conductive rubber, this appears as a change in electrical resistance. Therefore, If we add a shear deformation to pressure conductive rubber as in Fig. 6-(c), the conduction routes fragment, and the number of conduction routes decreases. This situation show the electrical resistance to increase. the state in Fig. 6-(b) as in Fig. 6-(c), the internal state of the rubber, namely the conduction routes, fragments, and the number of conduction routes decreases, resulting in an increase in the electrical resistance. When the deformation stops, as in Fig. 6-(d), the conduction routes inside the rubber are restored. So, the electrical resistance seems to gradually decrease and returns to the former state.

*2) Speed of Rubber Shear Deformation:* Here we shall discuss the relationship between the shear deformation speed of the pressure conductive rubber and the change of voltage between the electrodes. As shown in Table I, the size of the voltage difference $\Delta V$ changes according to the deformation speed of the rubber. This change tends to be significant as the

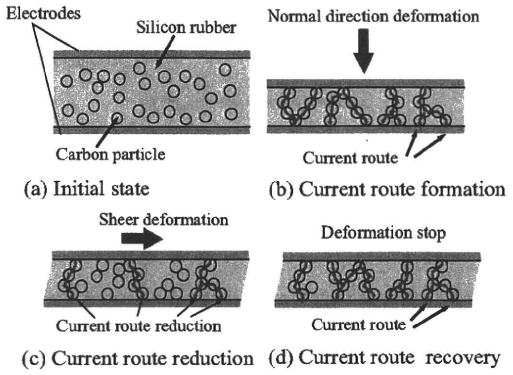


Fig. 6. Structure of Pressure conductive rubber

deformation speed becomes greater. Accordingly, the shear deformation speed was varied at appropriate intervals from 0.01 $mm/s$ to 10 $mm/s$, and the new voltage differences were measured. The voltage differences $\Delta V$ for each shear deformation speed plotted in a graph are shown in Fig. 7. This graph showed a nonlinear increase in voltage difference $\Delta V$ accompanying increases in the shear deformation speed ($v_s$) of the rubber. Regarding the conductive mechanism of pressure conductive rubber, the following items are to be considered. With slow shear deformation, only deviation in the conduction routes is produced and they are not fragmented. Meanwhile, with rapid deformation, conduction routes that were not fragmented with slow deformation are broken due to the sudden deformation. Therefore, the voltage difference $\Delta V$ increased more with rapid shear deformation.

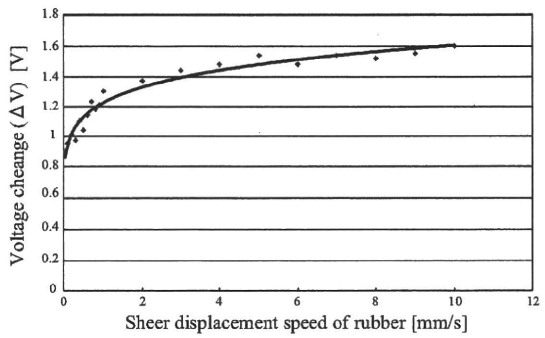


Fig. 7. Relation between voltage change $\Delta V$ and sheer displacement speed

## V. Summary

To investigate the slip detection properties of the CoP sensor, an experiment comparing the outputs of a load cell and CoP sensor was conducted. The results showed that the CoP load output varied with slip of the object being gripped. This change was more sensitive than alaser displacement sensor (resolution 0.1 $mm$), and so it could be utilized to detect the initial slip. An experiment in which pressure conductive rubber was made to undergo a shear deformation was also conducted to clarify the CoP sensor slip detection mechanism. We found that when the pressure conductive rubber underwent a shear deformation, the resistance greatly increased. It was made clear that the load output change of CoP sensor depends on the special properties of pressure conductive rubber.

It is suggested that, through this experiment, the slip sensor without the CoP sensor could be configured using pressure conductive rubber. For example, when the simplest structure of pressure conductive rubber sandwiched between two electrodes is used, as in this experiment, the object is set on the sensor, made to slip, and simultaneous with it slipping, the potential across the electrodes changes. By measuring this change, it is possible to detect slippage. When pressure conductive rubber is utilized to configure a slip sensor, considering the special properties, it will have the following characteristics.

Since the pressure conductive rubber is thin, approximately 0.5$mm$, and light, so even with the electrodes are attached, a thin, lightweight sensor can be configured. Since there is a change in the potential across the electrodes with a shear deformation of only 0.01$mm$ as shown in the shear deformation experiment, it is of extremely high sensitivity.

The sensor has a high speed responsibility. Since the voltage is held constant during the shear deformation of the pressure conductive rubber (Fig. 5), detection is possible in the course of the object slipping. As shown in section IV-.2, if the speed of shear deformation of the rubber ($V_s$) and the speed of slippage of the object are set equal, the slip speed of the object can be detected from the potential difference ($\Delta V$) at the time of the shear deformation and the initial potential ($V_i$). In this paper, we proposed highly sensitive slip sensor which can be configured of pressure conductive rubber and electrodes, we will conduct more detailed experimental analysis regarding the properties of pressure conductive rubber, and apply it to slip sensors.

## References

[1] Noriatsu Furukawa, Akio Namiki, Taku Senoo and Masatoshi Ishikawa, *Dynamic Regrasping Using a High-speed Multifingered Hand and a High-speed Vision System*, Proc. IEEE Int. Conf. on Robotics and Automation, pp.181-187, 2006

[2] H. Kawasaki, T. Komatsu, K. Uchiyama, *Dexterous Anthropomorphic Robot Hand With Distributed Tactile Sensor : Gifu Hand II*, IEEE/ASME Trans. Mechatronics, Vol7, No.3, pp.296-303, 2002

[3] M.R. Trembly, M.R. Cutkosky, *Estimating Friction using Incipient Slip Sensing During a Manipuration Task* , Proc. IEEE Int. Conf. on Robotics and Automation, pp.429-434, 1993

[4] J.S. Son, E.A. Monteverde and R.D. Howe, *A Tactile Sensor for Localizing Transient Events in Manipulation*, Proc. IEEE Int. Conf. on Robotics and Automation, pp.471-476, 1994

[5] Y. Koda, T. Maeno, *Grasping Force Control in Master-Slave System with Partial Slip sensor*, Proc. IEEE/RSJ Int. Con. on Intelligent Robots and Systems, pp.4641-4646, 2004

[6] H. Shinoda, S. Sasaki, K. Nakamura, *Instantaneous Evaluation of Friction based on ARTC Tactile Sensor*, Proc. IEEE Int. Conf. on Robotics and Automation, Vol.3, pp.2173-2178, 2000

[7] M. Ishikawa, M. Shimojo, *A Method for Measuring the Center Position of a Two Dimensional Distributed Load Using Pressure-Conductive Rubber*, SICE Trans. vol.18, no.7, pp.730-735, 1982 (in Japanese)

[8] D. Gunji, Y. Mizoguchi, S. Teshigawara, A. Ming, A. Namiki, M. Ishikawa, M. Shimojo, *Grasping Force Control of Multi-fingered Robot Hand Based on Slip Detection Using Tactile Sensor*, ICRA 2008 (in press)

2008 IEEE International Conference on
Robotics and Automation
Pasadena, CA, USA, May 19-23, 2008

# Grasping Force Control of Multi-fingered Robot Hand based on Slip Detection Using Tactile Sensor

Daisuke Gunji***, Yoshitomo Mizoguchi*, Seiichi Teshigawara*,
Aiguo Ming*, Akio Namiki**, Masatoshi Ishikawaand** and Makoto Shimojo*

*Abstract*— **To achieve a human like grasping with a multi-fingered robot hand, the grasping force should be controlled without using information from the grasped object such as its weight and friction coefficient. In this study, we propose a method for detecting the slip of a grasped object using the force output of Center of Pressure (CoP) tactile sensors. CoP sensors can measure the center position of a distributed load and the total load applied on the surface of the sensor, within 1 ms. These sensors are arranged on the fingers of the robot hand, and their effectiveness as slip detecting sensors is confirmed in tests of slip detection during grasping. Finally, we propose a method for controlling grasping force to resist tangential force applied to the grasped object using a feedback control system with the CoP sensor force output.**

## I. INTRODUCTION

In order for robots to achieve the same level of precision in manual operation that humans achieve, many researchers are working on highly versatile, multi-fingered robot hands that offer a high degree of freedom. A typical operation of hands is grasping objects. In the past, since it was assumed that robots would grasp specific objects, it was sufficient to use a simple gripper structure as a hand, and to set its grasping force to the required value. However, since each grasped object has a different coefficient of friction and weight, to achieve human-like grasping, it is necessary to set the grasping force appropriately for each object without being aware of this data in advance. Moreover, in order to grasp objects without damaging them, it is desirable to grasp them with the minimum force without slip. Various slip sensors have been proposed to achieve this kind of grasping ability [1].

In human grasping, Johansson et al [2][3] showed that localized slip between the skin and the grasped object is an important factor in adjusting grasping force. Maeno et al [4][5] proposed an elastic finger for distributed sensing using strain gauges with a curved surface, and showed that by imitating the method of grasping objects used by humans, it is possible to pick up any object for which the weight and friction coefficient is not known, at any speed. However, this approach involves the disadvantages of having to produce dedicated fingers, and the requirement for many strain amplifiers to support the arrays of strain gauges. Melchiorri [6] has proposed a method of controlling grasping force by detecting translation and rotational slip using force/torque sensors based on strain gauges, and distributed tactile sensors. However, with this approach the static friction coefficient of the object must be known. Furthermore, since distributed tactile sensors are used, wiring them into the robot is a problem. Ikeda et al [7] have proposed a method of controlling grasping force by measuring the degree of eccentricity of the contact surface using a camera. With methods such as this using vision, how to incorporate cameras in relatively small places such as hands is a problem. Furthermore, processing speed depends on the frame rate of vision, and it is generally difficult to achieve slip detection at high speeds.

This paper shows an approach to slip detection using thin, flexible, lightweight two-dimensional center of pressure tactile sensors (Center of Pressure sensors, hereafter "CoP sensors") [8][9] that can be mounted on a robot hand. CoP sensors can measure the center position of a distributed load applied to the surface of the sensor and the total load itself within 1(ms). Thus, rapid slip detection can be achieved. Furthermore, only four wires are needed, irrespective of the size of the sensor area, making it easy to mount them on a robot hand. This paper describes slip detection tests using CoP sensors and shows that slip can be detected immediately before it occurs based on the force output of the CoP sensors. Next we show that when force is added to a grasped object causing slip, it is possible to achieve grasp control to resist the force using a force control system with feedback from the force output of the CoP sensors. Finally we propose a method of grasping with optimal grasping force for the object even when its friction coefficient is not known, by adjusting the grasping force based on slip detection using the output of the CoP sensors.

## II. STRUCTURE AND FEATURES OF THE SENSOR

### A. Structure and Features of the CoP Sensor

CoP sensors can measure the center position of a distributed load and the total load itself [8][9]. The structure of the CoP sensor, as shown in Fig.1, consists of pressure sensitive material sandwiched between two sheets of conductive film, Layers A and B (upper and lower layers respectively). Both edges of the conductive film are electrodes, and we can derive the center position of the current distribution from the potential difference of the electrodes on both conductive film layers. Considering the pressure characteristic of pressure conductive material, it is possible to regard the center position of the current distribution as the center position of

*Graduate School of Electro-Communications, The University of Electro-Communications.
**Graduate School of Information Science and Technology, The University of Tokyo.
***NSK Ltd, Emerging Techonologies R&D Department.

978-1-4244-1647-9/08/$25.00 ©2008 IEEE.

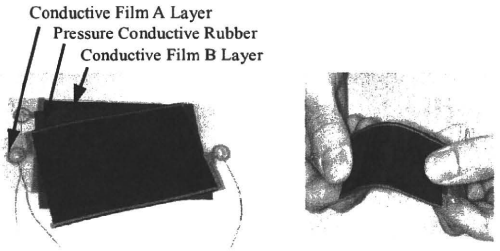


Fig. 1. Structure of CoP Sensor

the load distribution, and the total current which flows circuit as the total load applied to the sensor.

Since CoP sensors consist of thin and flexible materials, they can be used arranged on curved surfaces. Furthermore, they find the center position of load distribution using the potential difference of the electrodes on both conductive film layers, so only four wires are required for the sensors, irrespective of their area, ensuring compact wiring. That is to say, CoP sensors have features that suit them to mounting on robot hands.

The arithmetic processing of the CoP sensors is achieved with simple analog circuits alone. Therefore, the time taken for calculation is very short, thereby achieving a high-speed response within 1(ms). Thus the sensors can be used directly in control loops of 1(kHz).

*B. Output Characteristics of CoP Sensor*

*1) Position and Total Force Output:* The position and the total force output characteristics of CoP sensor are shown in Fig.2 and Fig.3 respectively, when arranged on cylinder with diameters of 18(mm) equivalent to the finger-tip of the hand to use for an experiment. The point where pressure is applied and the output voltage of the sensor are in proportional relationship. The results show that as the pressure applied increases, the output of the sensor increases. In addition, with increasing and decreasing pressure the output differs, demonstrating hysteresis properties.

*2) Slip Detection:* We inspected behavior for tangential force of CoP sensor with the experimental system as shown in Fig.4.Firstly, the two fingers of the hand with the CoP sensors grasped an object.After grasping the object starts,

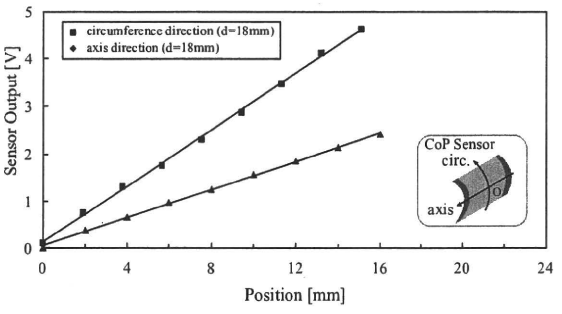


Fig. 2. Position output characteristics

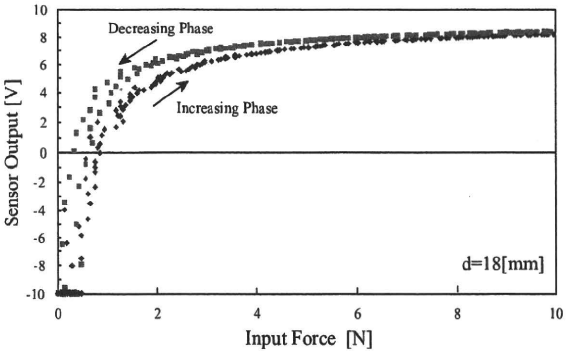


Fig. 3. Total force output characteristics

the hand was made to maintain the same joint angle. The grasped object is connected to a DC motor by a wire, and was started to slip vertically downwards due to rotation of the DC motor. Vertical slip displacement of the grasped object was measured with a laser displacement sensor (Omron: ZX-LDA11-N) above the object. The outputs of the sensor and laser displacement sensor were input into a computer via an AD board (Interface: PCI-3168). The control cycle of the hand and the sensor output sampling cycle was 1(ms).

The results of the tests are shown in Fig.5. The figures show the slip displacement of the grasped object measured with a laser displacement sensor and the CoP sensor output (force output and position output). The change in CoP sensor position output due to the occurrence of slip is small with a maximum of 0.3(V). Immediately before slip displacement occurs, the total force output of the CoP sensors falls significantly (the shaded area of sensor force output in Fig.5). Thereafter at the stage where slip displacement is happening, the force output increases again, and during slip, complex changes are indicated. Since these characteristics may change depending on covering material, we performed the same experiment about some materials. As a result, the almost same characteristic was confirmed for all materials. Thus, It

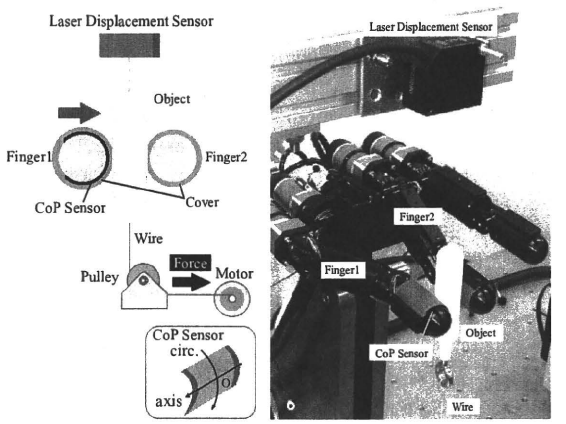


Fig. 4. Experimental system of slip detection on grasping

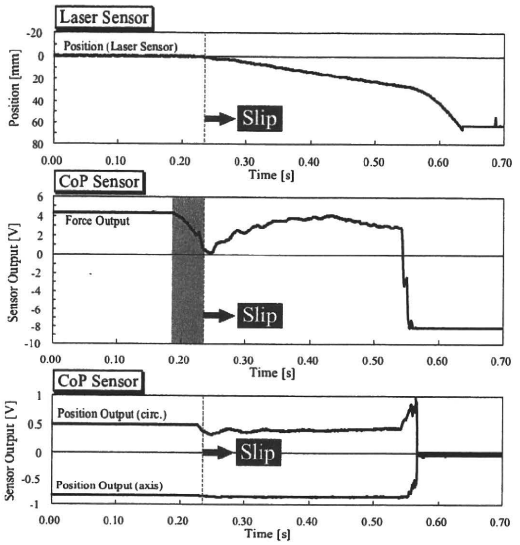


Fig. 5. Experimental result of slip detection on grasping

is thought that falling of total force output of CoP sensor can use slip detection.

## III. Multi-fingered robot hand

In this research we used the high-speed three-fingered hand developed by Namiki et al [10]. This hand has three finger modules with two degrees of freedom, and it comprises joints that swivel the fingers on both sides. The finger modules incorporate an AC servomotor, harmonic drive, and encoder for driving the joints, and each joint is driven with a bevel gear.

Although small and light, this hand can open and close 180 degrees in 100(ms). In addition, it achieves high instantaneous output, obtaining greater grasping force than earlier hands. Furthermore, the hand has the superior characteristic in that backrush in the fingers overall is almost 0.

The maximum torque of the fingertip joints of the finger modules is 0.35(Nm), while that of the basal joints and swivel joints is 2.65(Nm). The control system feeds back the current target joint angle in relation to the target joint angle and sends commands regarding the torque of each joint using PD control. The control system was built on a PC with ART-Linux (kernel-2.4.22-0vl2.11ART) as the OS. The control cycle is 1(ms).

CoP sensors were mounted on each joint of the finger modules. The method used to mount the sensors on the finger modules is shown in Fig.6.

## IV. Control of a multi-fingered robot hand to resist slip

### A. The Basic Concept behind Grasping Force Control

From the test results in Section II-B.2, it is clear that immediately before slip displacement occurs, the CoP sensors show changes in force output. Using this characteristic, we propose a method of control in which grasping force

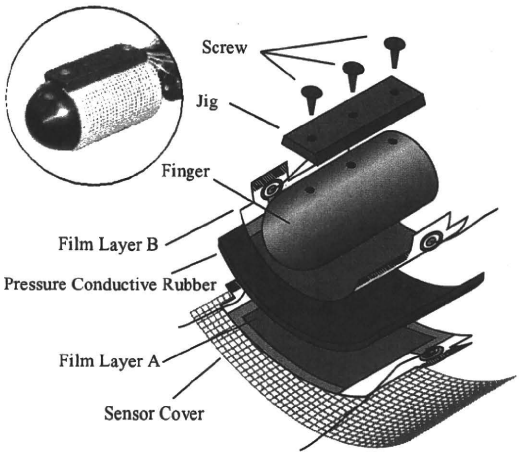


Fig. 6. Installation of CoP sensor

is increased when tangential force causing slip is detected. Hereafter, we will call the proposed control system anti-slip control.

In the test described in Section II-B.2, vertical downward force was applied to the grasped object therefore there should be no change in normal force even at the stage when CoP sensor force output is changing. That is to say, force output of the CoP sensors actually shows a smaller value than for normal force. In relation to this, we considered control that achieves a certain sensor force output. If the sensor force output falls due to the occurrence of slip, control works to increase the force output. As a result, it is supposed that as an amount of slip force increases, the grasping force also increases through control.

In other words, with only a force control system that feeds back the CoP sensor force output, grasping force control that resists tangential force without any special control should be possible.

The proposed anti-slip control can be achieved with just a simple force control system, and no information about the grasped object whatsoever is required. However, if there is no margin in the target grasping force for the limits of friction, or if strong tangential force is applied, it is possible that increased grasping force from the control system will be insufficient and slip will occur.

### B. Control System

As described in the previous section, with only a force control system that feeds back the CoP sensor force output, grasping force control that resists tangential force is possible. So damping control as shown in formula (1) was added to the PD control of the joint angle of the hand as anti-slip control.

$$\theta_{\mathrm{ref}} = \hat{\theta}_{\mathrm{ref}} + \hat{A} \int (V_{\mathrm{ext}} - V_{\mathrm{ref}})\, dt \qquad (1)$$

Here, $\hat{\theta}$ is the target joint angle, $\hat{A}$ is the coefficient, $V_{\mathrm{ext}}$ is the CoP sensor force output, $V_{\mathrm{ref}}$ is the target value for sensor force output, and $\theta_{\mathrm{ref}}$ is the new target joint angle. Normally,

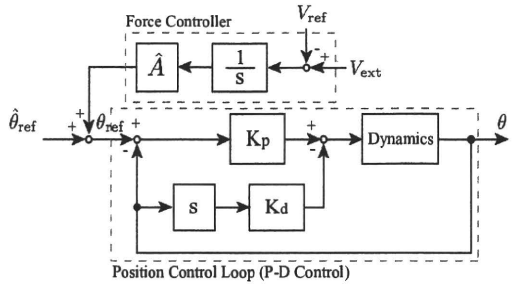


Fig. 7. Control system of muti-fingered robot hand

the force output of the CoP sensors and the relevant target values should be converted from voltage levels to force, but here for the sake of simplicity, the voltage levels themselves are used as is. Also for simplicity's sake, the position of the hand is not considered. Fig.7 shows the configuration of the control system.

### C. Test Method

The hand grasped an object and when tangential force was applied to the grasped object, changes in the grasping force were measured.

As shown in Fig.8 (a), an object with a load cell built into it was grasped by the fingertip joints of the hand.Anti-slip control was only applied to the basal joints of the fingers grasping the object. The target value of the sensor force output was $V_{\text{ref}} = 3.0(V)$.

After the object was grasped, tangential force was applied by human hand to the grasped object. As shown in Fig.8 (b), tangential force was applied to the grasped object from three different directions in the tests, from above, from below, and from the front.

### D. Test Result

Fig.9 shows the grasping force measured from the sensor force output and load cell with anti-slip control. The time shown shaded in the figure is when tangential force is applied. Furthermore, the numbers shown in circles indicate the direction of tangential force, corresponding to Fig.8(b). Irrespective of the direction in which the tangential force is applied, it is apparent that the load output of the CoP sensors falls significantly at the same time as tangential force is applied.

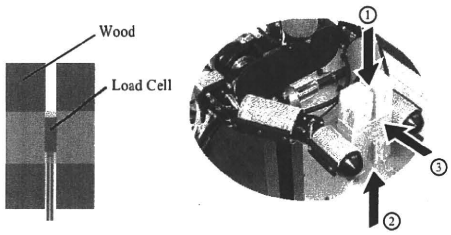


(a) Grasping object (b) Tangential force direction

Fig. 8. Experimental result (without anti-slip control)

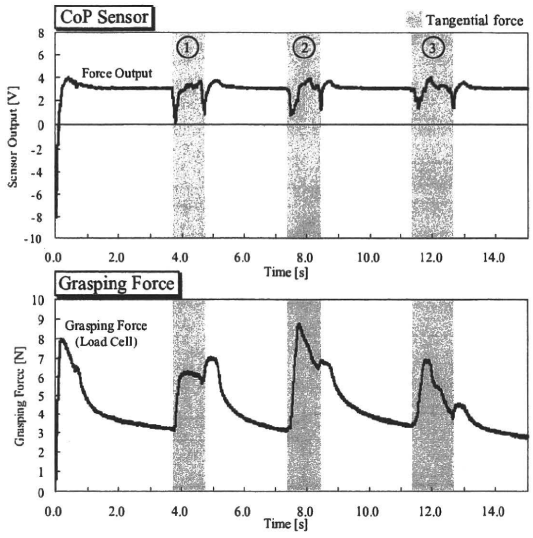


Fig. 9. Experimental result (top:without anti-slip control / bottom:anti-slip control)

When anti-slip control is applied, grasping force increases significantly as soon as tangential force is applied. Furthermore, it is apparent that in all cases grasping force increases, irrespective of the direction of tangential force.

Therefore, the speed at which grasping force increases, in other words the responsiveness to the application of tangential force, changes with the gain of the control system. The influence of integration gain $\hat{A}$ in particular can be thought to be significant. The greater $\hat{A}$ is, the faster the response, but there is a greater possibility that instantaneous grasping force will be excessive, breaking the object.

The results of the tests show that with simple force control that feeds back the CoP sensor force output, it is possible to achieve grasping force control that resists tangential force.

## V. Multi-fingered Robot Hand Grip Control Based on Slip Detection

### A. Basic Concept

As one of the necessary sufficient conditions for a multi-fingered robot hand to be able to grasp an object in a still state there exists the condition that the power of each fingertip of the hand is within the friction cone [11]. Based on this, it is possible to prevent slip if control is performed so that fingertip power always remains within the friction cone. However, for this control a static friction coefficient is required as a parameter. In order to avoid restrictions on the objects that can be grasped, an approach is required that allows control even when the static friction coefficient is unknown. Therefore this paper proposes a method of control in which appropriate grasping force for the grasped object can be achieved even when the coefficient of friction and weight of the grasped object are unknown, using the force output of CoP sensors.

The basic concept of the proposed approach is as follows. When a hand grasps an object, if the grasping force is

too weak, the object will slip. However, if this slip is detected and the grasping force is increased slightly, when the required grasping force is reached, slip no longer occurs. In the above process, all that is required is detection of slip and a corresponding increase in grasping force, and no information about the grasped object is required whatsoever. This approach is similar to the control method that humans may be supposed to use.

From the test results in Section II-B.2, it is clear that immediately before slip displacement of the grasped object occurs, the force output of the CoP sensors falls. Therefore, we propose a control method that regards this change in output as occurrence of slip, and increases the grasping force with a target in accordance with the occurrence of slip. With the proposed method, grasping force is controlled based only on sensor output, so no information about the grasped object such as the coefficient of friction is required whatsoever. Furthermore, since changes in sensor output can be obtained immediately before slip displacement occurs, if the hand operates fast enough, it should be possible to adjust grasping force before slip displacement occurs in most cases.

### *B. Control Method*

The basic control system is the anti-slip control proposed in Section IV. Here, grasping force is adjusted by changing the target value for sensor force output $V_{\mathrm{ref}}$ in relation to the sensor output. Hereafter, we will simply call the target value for sensor force output $V_{\mathrm{ref}}$ the "target valu".

In the proposed method, a low value is first set for $V_{\mathrm{ref}}$, and grasping of the object starts. After grasping starts, $V_{\mathrm{ref}}$ is changed in accordance with formulas (2) and (3). $\Delta t$ is the control cycle.

When $V_{\mathrm{ref}}(t) - V_{\mathrm{ext}}(t) > V_{\mathrm{th}}$

$$V_{\mathrm{ref}}(t+\Delta t) = V_{\mathrm{ref}}(t) + K_{\mathrm{fp}}\{V_{\mathrm{ref}}(t) - V_{\mathrm{ext}}(t)\} \quad (2)$$

When $\dot{V}_{\mathrm{ext}} < c$ and $V_{\mathrm{ref}}(t) - V_{\mathrm{ext}}(t) > 0$

$$V_{\mathrm{ref}}(t+\Delta t) = V_{\mathrm{ref}}(t) - K_{\mathrm{fd}}\dot{V}_{\mathrm{ext}} \quad (3)$$

Here, $V_{\mathrm{th}}(>0)(V)$ and $c(<0)(V/s)$ are appropriate threshold values, and $K_{\mathrm{fp}}$ and $K_{\mathrm{fd}}$ are coefficients.

It can be said that the smaller the threshold value $V_{\mathrm{th}}$ and c in each conditions, the greater the sensitivity to slip. However, if the threshold value is too low, even if slip is not occurring, the target value will be increased, and the grasping force will be excessive. In addition, since the bigger the coefficients $K_{\mathrm{fp}}$ and $K_{\mathrm{fd}}$, the faster the target value is increased, it is possible to reduce the occurrence of slip displacement, but at the same, the possibility that grasping force becomes excessive also increases. Therefore, it is necessary to set appropriate values for these parameters, taking into account the responsiveness of the multi-fingered robot hand used for grasping.

### *C. Test Method*

We tested the proposed control method on the multi-fingered robot hand, grasping an object for which the coefficient of friction and mass were unknown. The experimental system is shown in Fig.10.

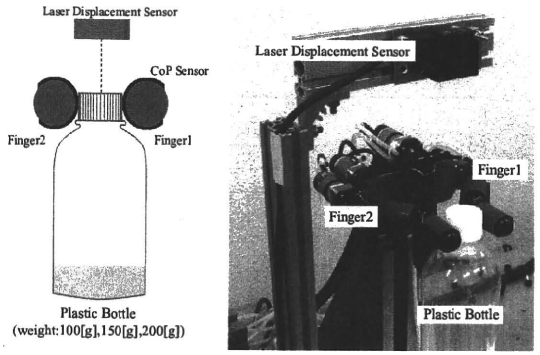


Fig. 10. Experimental system of grasping force control

The grasped object is a plastic bottle with water in it. By changing the amount of water in the bottle, its weight was set at 100(g), 150(g), and 200(g), and testing was conducted with each weight. Slip displacement of the bottle was measured with a laser displacement sensor (Omron: ZX-LDA11-N) above the object. The outputs of the sensor and laser displacement sensor were input into a computer via an AD board (Interface: PCI-3168). The control cycle of the hand and the sensor output sampling cycle was 1(ms).

First, the robot hand was made grasp the plastic bottle held by a human. After the hand grasped the bottle, the human let go of it so that only the hand was holding it.

Grasping control was only applied to the basal joints of the fingers grasping the bottle. Slip-resistant mesh (approx. 1(mm) lattice, thickness 0.5(mm)) was used to coat the surface of the sensors. The initial target value was $V_{\mathrm{ref}} = 6.0$(V). The sensor force output voltage when unloaded was -8.0 V. The various parameters were $V_{\mathrm{th}} = 1.0$(V), $c = -30.0$(V/s), $K_{\mathrm{fp}} = 3.0 \times 10^{-3}$, and $K_{\mathrm{fd}} = 5.0 \times 10^{-4}$.

Separately from the above test, we also examined the minimum grasping force that can be used to grasp the same object as in the test above without slip, in order to evaluate the proposed control method. Using the anti-slip control proposed in Section IV, we repeatedly changed the target value Vref in increments of 0.5 V for each weight of the grasped object until the hand grasped it without slip. The results for the minimum necessary grasping force were target values of -1.5 V (100 g), 1.0 V (150 g), and 3.5 V (200 g) respectively.

### *D. Test Results*

Fig.11 shows the slip displacement of the grasped object with weight of 100(g), the sensor force output, and the target value. Table I shows the grasped object with weights of 150(g) and 200(g), with the target grasping force at the point when stable grasping was achieved $V_{\mathrm{ref}}$(V), the minimum necessary grasping force $V_{\mathrm{ref}}$ (Min) (V), the displacement that occurred up to stable grasping, and the time required up to that point.

The results of the test show that for all weights of object, grasping force was adjusted in accordance with the weight of the object using the proposed control method. When slip

TABLE I

EXPERIMENTAL RESULT OF GRASPING FORCE CONTROL

| | Weight | | |
|---|---|---|---|
| | 100 (g) | 150 (g) | 200 (g) |
| $V_{ref}$ (V) | -0.24 | 1.4 | 3.7 |
| $V_{ref}$ (Min) (V) | -1.5 | 1.0 | 3.5 |
| Slip (mm) | 0.54 | 1.4 | 2.5 |
| Adjustment time (s) | 0.60 | 1.09 | 0.83 |

displacement and sensor force output are compared, the force output of the sensors falls significantly when slip displacement occurs, and the target value is increased accordingly. Furthermore, in all cases, adjustment of grasping force was performed in about 1(s). The slip displacement from the start of grasping to stable grasping is 0.5(mm) (100(g)), 1.4(mm) (150(g)), and 2.5(mm) (200(g)) respectively, and the heavier the object, the greater the slip displacement that occurs before stable grasping is achieved.

### E. Discussion

Regarding the stable grasping state in the test results, when the target values obtained with the proposed control method and the minimum grasping force found in other tests are compared, the values are somewhat greater for objects of 100(g), but with objects of 150(g) and 200(g), values that largely match were obtained. Furthermore, the time required from the start of grasping to when grasping force was adjusted and stable grasping was achieved is short at 1(s). Even under the stringent conditions in this test when the object was passed in midair and the force was changed suddenly, stable grasping was achieved with relatively little slip displacement.

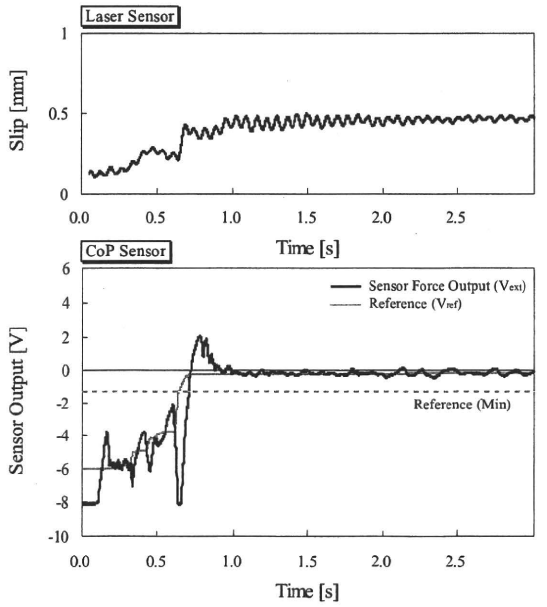


Fig. 11. Experimental result of grasping force control (weight:100g)

## VI. CONCLUSIONS AND FUTURE WORKS

### A. Conclusions

In this paper we proposed an anti-slip control method using these characteristic force output changes, and confirmed the effectiveness of the proposed method through testing. Furthermore, we proposed a method of adjusting grasping force in response to slip detected using sensor force output, and in testing using the proposed method, we showed that optimum grasping force can be obtained even when no information about the grasped object is known.

### B. Future Works

The reasons for the occurrence of the characteristic changes in sensor force output immediately before slipping occurs must be clarified. In addition, by covering the sensor surface with appropriate material, it should be possible to infer the direction of slip of an object from changes in the sensor position output. We will confirm these matters in future testing.

This paper describes tests with a relatively simple grasping position, but the proposed control method can probably also be applied to more complex grasping positions such as power grasps. Therefore in future we will examine control methods that take grasping position into consideration, with the aim of achieving dexterous grasping similar to that of humans.

## REFERENCES


[1] Y.Yamada, "Sensing Strategies before Grasping Part 2 Detection of Slip and Static Friction Coefficient Used to Acquire Information on Surface Roughnes", *Journal of the Robotics Society of Japan*, vol.11, no.7, pp.959-965, 1993.

[2] R.S.Johansson, G.Westling, "Roles of glabrous skin receptors and sensorimotor memory in automatic control of precision grip when lifting rougher or more slippery objects", *Exp Brain Res*, vol.56, pp.550-564, 1984.

[3] R.S.Johansson, G.Westling, "Signals in tactile afferents from the fingers eliciting adaptive motor responses during precision grip", *Exp Brain Res*, vol.66, pp.141-154, 1987.

[4] T.Maeno, S.Hiromitsu, T.Kawai, "Control of Grasping Force by Estimating Stick/Slip Distribution at the Contact Interface of an Elastic Finger Having Curved Surface", *Journal of the Robotics Society of Japan*, vol.19, no.1, pp.91-99, 2001.

[5] T.Kawai, Y.Hirano, T.Maeno, "Development of Strain Distribution Sensor Having Curved Surface for Grip Force Control", *The Japan Society of Mechanical Engineers.C*, vol.64, No.627, pp.4264-4270, 1998.

[6] Claudio Melchiorri, "Slip Detection and Control Using Tactile and Force Sensors", *IEEE /ASME Transaction on Mechatronis*, vol.5, no.3, pp.235-243, 2000.

[7] A.Ikeda, Y.Kurita, J.Ueda, Y.Matsumoto, T.Ogasawara, "Grip Force Control of the Elastic Body based on Contact Surface Eccentricity During the Incipient Slip", *Journal of the Robotics Society of Japan*, vol.23, no.3, pp.337-343, 2005.

[8] M.Ishikawa, M.Shimojo, "A Method for Measuring the Center Position of a Two Dimensional Distributed Load Using Pressure-Conductive Rubber", *The Society of Instrument and Control Engineers*, vol.18, no.7, pp.730-735, 1982.

[9] M.Shimojo, T.Araki, A.Ming, M.Ishikawa, "A ZMP Sensor for a Biped Robot", *Proc. IEEE Int. Conf. Robotics and Automation CD-ROM*, pp.1200-1205, 2006.

[10] A.Namiki, Y.Imai, M.Ishikawa and M.Kaneko, "Development of a High-speed Multifingered Hand System and its Application to Catching", *Proc.of IEEE/RSJ Int.Conf.on Intelligent Robots and Systems*, pp.2666-2671, 2003.

[11] T.Yoshikawa, Y.Yokokohji, A.Nagayama, "Object Handling by Tree-Fingered Hand Using Slip Motion", *Journal of the Robotics Society of Japan*, vol.10, no.3, pp.394-401, 1992.

社団法人 電子情報通信学会
THE INSTITUTE OF ELECTRONICS,
INFORMATION AND COMMUNICATION ENGINEERS

信学技報
IEICE Technical Report
NC2008-56(2008-10)

# 義手制御に向けた針筋電信号による手指状態推定
## 単収縮モデルを用いた推定手法の提案

橘 秀幸† 鈴木 隆文† 満渕 邦彦†

† 東京大学大学院 情報理工学系研究科, 〒 113-8656 東京都文京区本郷 7-3-1
E-mail: †{tachibana@hil.t.u-tokyo.ac.jp, t.suzuki@i.u-tokyo.ac.jp, Kunihiko_Mabuchi@ipc.i.u-tokyo.ac.jp}

**あらまし** 本研究では，義手制御に向けて，針筋電信号を筋の単収縮を模したモデルへ入力することによって，指の筋の張力の推定を行なう手法の提案と，実験データによる有効性の実証を行なった．
**キーワード** 単収縮，筋電義手，針筋電信号，2 次系

# Estimation of finger state using needle EMG for the control of artificial hand
## –Proposal of an estimation method using single twitch contraction model–

Hideyuki TACHIBANA†, Takafumi SUZUKI†, and Kunihiko MABUCHI†

† Graduate School of Information Science and Technology, The University of Tokyo
7–3–1 Hongo, Bunkyo-ku, Tokyo, 113–8656 Japan
E-mail: †{tachibana@hil.t.u-tokyo.ac.jp, t.suzuki@i.u-tokyo.ac.jp, Kunihiko_Mabuchi@ipc.i.u-tokyo.ac.jp}

**Abstract** In this study, for the control of an artificial hand, we propose an method for estimating muscular tension of fingers by inputting needle EMG signals into the second order system which imitates muscle twitch contraction, and verify the effectiveness of the method by the experimental data.
**Key words** twitch, EMG prosthesis, needle EMG, second order system

## 1. はじめに

事故や疾病により手を失った患者は，厚生労働省の調査 [1] によると 2001 年現在日本国内におよそ 98,000 人いるとされる．これらの上肢切断患者では，失った腕の外観や機能を補うために義手を装着するなどの方法が取られている．特に機能に重点を置いたものとして，近年では生体信号を用いて義手を制御する方法が研究されている．

このとき用いる生体信号としては，神経信号と筋電信号の 2 種類が考えられる．神経信号は，脳の運動野から発せられた信号が筋まで伝えられるより前の地点で計測したもので，中枢神経信号と，末梢神経信号とがある．いずれの場合も，完全な神経信号が得られれば，それを適切なモデルへ入力することによって原理的には手の動作を完全に推定することができると考えられる．一方，筋電信号は，神経信号が神経筋接合部まで伝わったときに筋線維に生じる活動電位であり，それを計測したものを筋電図 (EMG; electromyogram) と呼ぶ．筋電信号には，筋線維から直接計測した針筋電信号 (nEMG; needle EMG) と，皮膚の表面で計測した表面筋電信号とがある．筋電信号は，筋の状態と高い相関関係があることや，神経信号と比べて計測が容易であることから，よく用いられる．筋電信号を用いて制御する義手は筋電義手と呼ばれ，一部では実用化されているが，指の繊細な動作など，手の本来の機能を補うまでには至っていない．

義手の制御においては，各関節の角度および角速度を各時刻で適切に決定する必要がある．関節の角度と角速度は，対立する筋の張力の釣り合い関係によって決まるため，筋の張力を推定することは義手の制御のための重要な基礎である．筋電信号を用いた筋の張力の推定としては，ニューラルネットワークや AR モデルなどの統計的手法を用いた研究が知られているが，これらの手法の推定精度はまだ十分とはいえず，新しい方法が求められている．

そこで本研究では，筋の生理学的なモデルを基本とした手法を検討する．筋のモデルとしては，Hill のモデルや Hatze のモデルが知られており，Hatze のモデルを用いて手の動作の推定を行った研究では，Watanabe ら [2] による機能的電気刺激に